

(Figs. 2a and 2b). The additional magnetization of the ferrite IIB is frequency-dependent, similar to that of ferrite I.

Distortion measurements have also been carried out on transformers having these ferrite cores. The distortion gradually decreases with frequency and reaches zero at the frequency where B is a linear function of H .

From these results it is concluded that in ferrites with a high permeability, at magnetic field strengths of about H_c , an additional magnetization process occurs which (a) is frequency-dependent already below the gyromagnetic resonance frequency, (b) takes place at a lower field strength as the density of the ferrite is greater, (c) is irreversible (since Rayleigh's law holds in small fields).

The initial permeability and the permeability at high frequencies, which is independent of the field strength, are, in our opinion, related to a pure rotational process. In contrast to the magnetization process giving rise to the above-mentioned permeabilities, the additional process is to be ascribed to irreversible Bloch-wall displacements in the ferrite. These results are contradictory to the conclusions reached by Rado *et al.*,⁵ that the initial permeability of ferrites is determined by reversible Bloch-wall displacements. A detailed paper on these experiments will be published shortly.⁶

¹ See J. L. Snoek, *New Developments in Ferromagnetic Materials* (Amsterdam, New York, 1947).

² J. L. Snoek, *Physica* **14**, 207 (1948).

³ D. Polder, *Proc. Inst. Elec. Engrs.* **97**, II, 246 (1950).

⁴ C. Kittel, *Revs. Modern Phys.* **21**, 541 (1949).

⁵ Rado, Wright, and Emerson, *Phys. Rev.* **80**, 273 (1950).

⁶ J. J. Went and H. P. J. Wijn, *Physica*, to be published.

Cross Section for the Reaction $C^{12}(\gamma, n)C^{11}$

R. N. H. HASLAM, H. E. JOHNS, AND R. J. HORSLEY
Department of Physics, University of Saskatchewan,
Saskatoon, Saskatchewan, Canada

(Received March 5, 1951)

THE cross-section curve for the reaction $C^{12}(\gamma, n)C^{11}$ has been determined by Baldwin and Klaiber.¹ However, in view of the discrepancy in the results obtained by these authors and the workers in our laboratory² for the reaction $Cu^{63}(\gamma, n)Cu^{62}$, the carbon cross section has been redetermined.

Carbon disks, 1.5 cm in diameter and 1.27 mm thick, were irradiated in a cavity in a Lucite block. The dose was monitored by an "r" meter placed in the same position. The resulting 20.6-min activity was counted in a fixed geometry. Figure 1 shows the

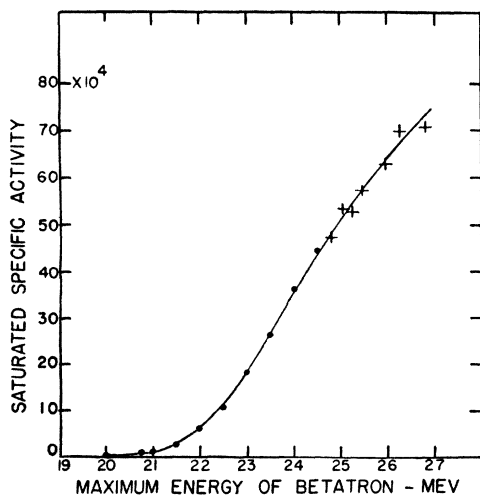


FIG. 1. Saturated specific activity in disintegrations per gram per 100 r as a function of maximum betatron energy, for the reaction $C^{12}(\gamma, n)C^{11}$. Corrections for geometry, etc., have been applied.

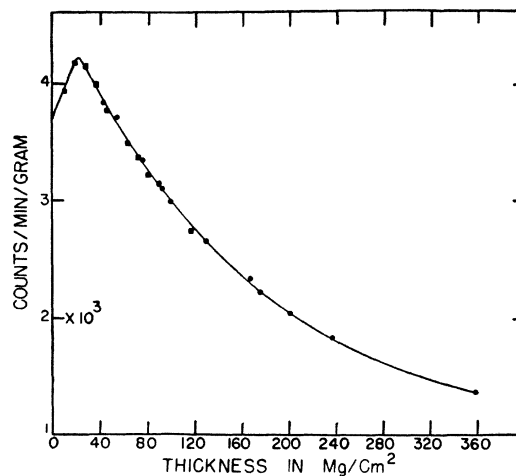


FIG. 2. Self-absorption curve for the positron activity of C^{11} .

saturated specific activity as a function of maximum betatron energy. Corrections for back-scattering, self-absorption, isotopic abundance, and geometry have been applied. The threshold for this reaction, assumed at 18.7 Mev,^{3,4} has been used as a calibration point for the betatron energy scale. No attempt has been made to show the portion of the activity curve between 18.7 and 20 Mev, although the contribution of this portion has been considered in the cross-section determination. The experimental points on the activity curve represented by circles were determined with the integrator circuit previously reported.³ The points marked with a cross were determined by the betatron panel meter. The two sets of results were brought into agreement by determining overlapping activity curves in the region 22 to 24 Mev.

As a check on some of the corrections applied in finding the saturated specific activity of carbon, copper and carbon samples were irradiated simultaneously at 23.5 Mev and counted in the same geometry. In determining the carbon activity, use was made of the results previously reported for copper² (lowered by 10 percent in agreement with more recent determinations). This latter method yielded a value for the saturated specific activity of carbon 5 percent higher than is reported here. This agreement is very satisfactory when one considers the possible errors involved.

The saturated specific activity curve has been used to determine the neutron yield at 22 Mev. The value obtained, 7.5×10^8 neutrons/mole/r, is in good agreement with the value 6.7×10^8 obtained by Price and Kerst.⁵

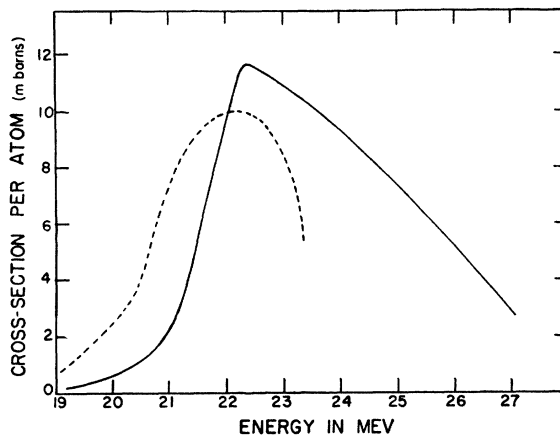


FIG. 3. Cross section vs energy curve for $C^{12}(\gamma, n)C^{11}$. The dotted curve shows the shape of the corresponding curve for $C^{12}(\gamma, p)B^{11}$ (reference 12).

Figure 2 is a self-absorption curve for the positron activity of C^{11} . Filter paper was used as a source of carbon for the points corresponding to small thickness (solid squares). The neglect of the bending-over of the curve would have led to an error of 20 percent in determining the activity at zero sample thickness. Similar, though larger, corrections were required for copper.

In Fig. 3 is shown the cross-section curve obtained from the activity curve by the method of analysis previously reported.² The cross-section curve has a peak value of 11.6 millibarns at 22.4 ± 0.5 Mev. The width at half-maximum is 4.25 Mev, and the integrated cross section is 0.047 Mev-barn. The ratio of the integrated cross sections of $Cu^{63}(\gamma, n)Cu^{62}$ ^{2,6} and $C^{12}(\gamma, n)C^{11}$ is $0.63/0.047 = 13.4$. This is in satisfactory agreement with ratios of the yields of these reactions produced by betatron x-rays of maximum energy 50 and 100 Mev (15.2, 14.4, respectively),⁷ and also with the ratio 14 given by Helmholtz and Strauch⁸ for 335-Mev x-rays. This would be expected if the cross sections for these reactions were negligible above 50 Mev. Our value of 0.047 Mev-barn for the integrated cross section is considerably lower than that obtained by Lawson and Perlman,⁹ who, however, assumed a sharp resonance occurring at approximately 30 Mev.¹

The average energy for the x-rays producing the $C^{12}(\gamma, n)C^{11}$ reaction, as obtained from absorption coefficient measurements, is given as 22.1 ± 1.5 Mev by Koch, McElhinney, and Cunningham¹⁰ and 25.3 ± 1.5 Mev by Marshall.¹¹ Although the peak of our cross-section curve lies at 22.4 Mev, the median ordinate lies at 23.5 Mev, and this probably corresponds more closely to the "average" photon energy obtained by the above authors.

The dotted curve of Fig. 3 shows the shape of the cross-section curve for the (γ, p) reaction in the same nuclide, as determined by Mann and Halpern.¹² It has been normalized to their minimum peak value of 1×10^{-26} cm². It is interesting to note that the maxima of the two curves occur at nearly the same energy.

The authors wish to thank Mr. A. Quinton for his assistance with many of the measurements involved. This work is supported by grants from the National Research Council and the National Cancer Institute of Canada. One of the authors (R.J.H.) is indebted to the Ontario Research Council for financial assistance.

¹ G. C. Baldwin and G. S. Klaiber, Phys. Rev. **73**, 1156 (1948).

² Johns, Katz, Douglas, and Haslam, Phys. Rev. **80**, 1062 (1950).

³ Katz, McNamara, Forsyth, Haslam, and Johns, Can. J. Research **A28**, 113 (1950).

⁴ McElhinney, Hanson, Becker, Duffield, and Diven, Phys. Rev. **75**, 542 (1949).

⁵ G. A. Price and D. W. Kerst, Phys. Rev. **77**, 806 (1950).

⁶ B. C. Diven and G. M. Almy, Phys. Rev. **80**, 407 (1950).

⁷ M. L. Perlman and G. Friedlander, Phys. Rev. **74**, 442 (1948).

⁸ A. C. Helmholtz and K. Strauch, Phys. Rev. **78**, 86 (A) (1950).

⁹ J. L. Lawson and M. L. Perlman, Phys. Rev. **74**, 1190 (1948).

¹⁰ Koch, McElhinney, and Cunningham, Phys. Rev. **81**, 318 (A) (1951).

¹¹ L. Marshall, Phys. Rev. **82**, 300 (1951).

¹² A. K. Mann and J. Halpern, Phys. Rev. **80**, 470 (1950).

Photoneutron Cross Sections of Fe^{54} , Ni^{58} , and Zn^{64}

L. KATZ, H. E. JOHNS, R. G. BAKER, R. N. H. HASLAM,
AND R. A. DOUGLAS

Betatron Group, University of Saskatchewan, Saskatoon,
Saskatchewan, Canada

(Received March 5, 1951)

THE photoneutron cross sections of Fe^{54} , Ni^{58} , and Zn^{64} have been investigated in this laboratory with the method outlined by the authors in an earlier paper.¹ The cross section *versus* energy curves are shown in Fig. 1, and the pertinent results are summarized in Table I. The threshold for the reaction in iron was also checked and was found to be in good agreement with values previously reported. Corrections to the observed activity for K capture amounted to 7 percent in the case of Zn^{64} ,² 100 percent in the case of Ni^{58} ,³ and 3 percent in the case of Fe^{54} . The last correction was estimated from the theoretical curves of Feenberg and Trigg,⁴ assuming the transition to be allowed.

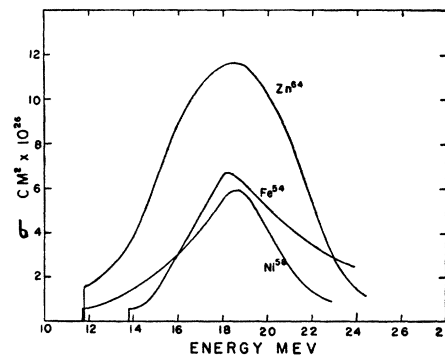


FIG. 1. Cross sections of Fe^{54} , Ni^{58} , Zn^{64} for (γ, n) reactions as a function of energy.

An examination of all published (γ, n) , (γ, p) , and (γ, d) cross sections would seem to indicate considerable similarity among them. For example, they all have half-widths of about 6 Mev, and their maximum cross sections, as previously pointed out by Katz and Penfold,⁵ occur about 6 Mev above the threshold (see also Table II). Fluctuations from this value are generally less than 1.5 Mev. Cameron⁶ analyzes the published neutron yield data on the basis of this similarity to obtain some interesting results. In addition, we would like to draw attention to the shape of the $Fe^{54}(\gamma, n)Fe^{53}$ and $C^{12}(\gamma, n)C^{11}$ curves. (See Haslam *et al.*⁷ for

TABLE I. Photoneutron cross-section data.

Parent isotope	Threshold Mev	Energy at peak cross section Mev	Maximum cross section barn	Half-width Mev	Integrated cross section Mev-barn
Fe^{54}	13.7 ± 0.2	18.3	0.067 ± 0.006	5.7	0.42
Ni^{58}		18.5	0.060 ± 0.006	4.6	0.33
Zn^{64}		18.5	0.12 ± 0.01	7.1	0.83

the latter curve.) These cross sections rise more steeply than the other curves; and after passing through a maximum value, they drop off relatively slowly, resulting in a long tail. We might infer from the behavior of these two isotopes that the relative position of the cross-section maximum and the threshold are not necessarily

TABLE II. Summary of photoneutron cross-section data.

Isotope and reaction	Threshold Mev	Energy at peak cross section Mev	Energy of peak cross section above threshold Mev	Reference
$C^{12}(\gamma, n)C^{11}$	18.7	22.4	3.7	a
$C^{12}(\gamma, p)B^{11}$	16	22.2	6.2	b
$Al^{27}(\gamma, n)Al^{26}$	14	19.6	5.6	c
$P^{31}(\gamma, n)P^{30}$	12.4	19	6.6	d
$S^{32}(\gamma, np)P^{30}$	19.1	25.8	6.4	d
$Fe^{54}(\gamma, n)Fe^{53}$	13.8	18.3	4.5	e
$Ni^{58}(\gamma, n)Ni^{57}$	12.0	18.5	6.5	e
$Cu^{63}(\gamma, n)Cu^{62}$	10.9	17.5	6.6	e
$Cu^{65}(\gamma, n)Cu^{64}$	10.7	19.0	8.5	e
$Zn^{64}(\gamma, n)Zn^{63}$	11.6	18.5	6.9	e
$Ag^{109}(\gamma, n)Ag^{108}$	9.3	16.0	6.7	f
$Ag^{109}(\gamma, p)Pd^{108}$	6.1		6.5	f
$Sb^{121}(\gamma, n)Sb^{120}$	9.3	14.5	5.2	e
$Sb^{122}(\gamma, n)Sb^{121}$	9.3	14.5	5.2	e
$Ta^{182}(\gamma, n)Ta^{180}$	8.0	13.5	5.5	e
Average 6.0				

^a Reference 7.

^b A. K. Mann and J. Halpern, Phys. Rev. **80**, 470 (1950).

^c To be published.

^d Reference 5.

^e Reference 1.

^f B. C. Diven and G. M. Almy, Phys. Rev. **80**, 407 (1950).